Drosophila Histone Deacetylase 6 Protects Dopaminergic Neurons against α-Synuclein Toxicity by Promoting Inclusion Formation

Guiping Du,*†‡ Xiang Liu,*‡ Xinping Chen,† Mei Song,† Yan Yan,†‡ Renjie Jiao,*† and Chih-chen Wang*

*National Laboratory of Macromolecules and †State Key Laboratory of Brain and Cognitive Science, Institute of Biophysics, Chinese Academy of Sciences, Beijing 100101, China; and ‡Graduate School of the Chinese Academy of Sciences, Beijing 100049, China

Parkinson's disease (PD) is associated with progressive degeneration of dopaminergic (DA) neurons. We report for the first time that the *Drosophila* histone deacetylase 6 (dHDAC6) plays a critical role in the protection of DA neurons and the formation of α-synuclein inclusions by using a *Drosophila* PD model constructed by ectopic expression of human α-synuclein. Depletion of dHDAC6 significantly enhances the effects caused by ectopic expression of α-synuclein, namely, loss of DA neurons, retinal degeneration, and locomotor dysfunction. Expression of α-synuclein in the DA neurons leads to fewer inclusions in the brains of *dHDAC6* mutant flies than in wild-type flies. Conversely, overexpression of dHDAC6 is able to suppress the α-synuclein–induced DA neuron loss and retinal degeneration and promote inclusion formation. Furthermore, mutation of *dHDAC6* reinforces the accumulation of oligomers that are suggested to be a toxic form of α-synuclein. We propose that α-synuclein inclusion formation in the presence of dHDAC6 protects DA neurons from being damaged by oligomers, which may uncover a common mechanism for synucleinopathies.

INTRODUCTION

As the second most common neurodegenerative disease, Parkinson's disease (PD) often impairs the sufferer's motor skills, speech, and other neuron-innervated functions (Jankovic, 2008). Neurodegenerative diseases are often featured as vulnerable neurons under misfolded protein stress (Taylor *et al.*, 2002). The prominent pathological characteristics of PD are progressive loss of dopaminergic (DA) neurons and emergence of proteinaceous inclusions named Lewy bodies (LBs). The major component of LBs is a small neuronal protein α-synuclein (Lang and Lozano, 1998), which is the first-identified genetic cause of PD (Polymeropoulos *et al.*, 1996, 1997). However, the link between α-synuclein and the neuron degeneration is not simply a matter of dosage of α-synuclein, although excess of this protein leads to higher cytotoxicity (Singleton *et al.*, 2003). The conformation of α-synuclein has also been shown to play an important role in the process of α-synuclein–induced neuron degeneration (Outeiro *et al.*, 2008). The oligomeric intermediates of α-synuclein aggregates are implicated to be the toxic species (Outeiro *et al.*, 2008). Despite of the establishment of PD models in flies (Feany and Bender, 2000), mice (Masliah *et al.*, 2000), and primates

(Kirik *et al.*, 2003), the detailed mechanism responsible for inclusion formation and α-synuclein neurotoxicity in vivo remains largely unclear.

Based on genetic studies of either inducing or suppressing PD pathological phenotypes, several genes have been identified to be involved in two types of PD pathogenesis. One type is autosomal recessive-juvenile Parkinson's (AR-JP) disease in which dopaminergic neuron loss is not associated with LB formation (Kitada *et al.*, 1998). The other type is autosomal dominant familial PD mainly caused by missense mutation in *α-synuclein* (Polymeropoulos *et al.*, 1997; Kruger *et al.*, 1998). In the latter case, the development of α-synuclein–induced PD is considered to be dependent on the forms and the dosage of α-synuclein (Singleton *et al.*, 2003). We set off to explore factors responsible for this complex event, and the relationship among the pathological hallmarks of Parkinson's disease.

The candidate factors relevant to the pathogenesis of PD should meet at least two criteria: 1) they must be modifiers (either suppressors or enhancers) of PD-like degenerative phenotypes; and 2) they must regulate α-synuclein aggregation, eventually its neurotoxicity. In this context, histone deacetylase 6 (HDAC6) possesses properties that place it on the top of the list. HDAC6 has been reported to rescue polyglutamine-mediated neurodegeneration in an autophagy-dependent manner (Pandey *et al.*, 2007). It senses ubiquitinated aggregates and consequently activates the expression of major chaperones, such as heat-shock protein (Hsp)70 and Hsp25 (Boyault *et al.*, 2007b). It directly facilitates aggresome formation via interacting with ubiquitinated proteins as a response to misfolded protein stress (Kawaguchi *et al.*, 2003), and its concentration determines the fate of ubiquitinated proteins (Boyault *et al.*, 2006). Here, we describe studies to investigate the physiological func-

tions of HDAC6 in PD pathogenesis by using the well established *Drosophila* PD model (Feany and Bender, 2000). Based on analyses of the *dHDAC6* null alleles generated with targeted gene knockout technique, our data reveal that dHDAC6 is a suppressor of α-synuclein–induced PD-like phenotypes in *Drosophila*. It promotes α-synuclein-enriched inclusion formation while reducing the oligomer form, a function that we suggest to be crucial for inhibiting the toxicity of α-synuclein. Our results provide a direct evaluation of the toxicity of different forms of α-synuclein during PD pathogenesis and highlight the role of dHDAC6 in handling the toxic α-synuclein forms by promoting them to become inclusions in vivo.

MATERIALS AND METHODS

Fly Stocks and Genetics

Flies were cultured under standard conditions at 25°C otherwise stated. Transgenic fly lines of *UAS-α-synuclein, UAS-mCD8::GFP, GMR-GAL4,* and *UAS-Prosbeta2¹* were obtained from the Bloomington Stock Center (Bloomington, IN). *TH-GAL4* line was a kind gift from Dr. Li Liu (The Institute of Biophysics, Chinese Academy of Sciences, Beijing, China). *TH-GAL4, UAS-α-synuclein/TM6B, Tb* flies were generated through recombining *TH-GAL4* transgene and *UAS-α-synuclein* transgene which are both on the third chromosome. To generate the *UAS-dHDAC6* construct, *dHDAC6* coding sequence which encodes 1128 amino acids referring to HDAC6-RA on the Flybase was amplified from wild-type *Drosophila* cDNA library and cloned into the *pUAST* vector. The final transformation construct was confirmed by DNA sequencing. P-element mediated germline transformation was performed using standard procedures.

Generation of dHDAC6 Mutant Flies

The *dHDAC6* genomic segment with intended modifications was cloned into the *pTARG* vector (Egli *et al.*, 2006) to make the gene targeting construct. Mutations were introduced with polymerase chain reaction (PCR) by changing AAAC⌐ATG⌐GT to AGATCT (dHDAC6 start codon is boxed). Primers used in this process were 5′-CAAC<u>AGATCT</u>GAGTACTGGCAGATTATTGCCG-3′ and 5′-TGAC<u>AGATCT</u>GTGGGATTTCGAGTTGGC-3′ (the restriction site is underlined). Mutation of AAACATGGT to *AGATCT* generates a new restriction site (BglII) for identification of mutant DNA. Oligonucleotides used to introduce I-SceI recognition site were AATTTAGGGATAACAGGGTAAT and AATTATTACCCTGTTATCCCTA. The donor plasmid was transformed into *Drosophila* by using standard procedures. The *dHDAC6* mutant flies were generated by "ends-in" targeting strategy (Rong and Golic, 2000). First, the donor transgenic flies were crossed to flies bearing heat-inducible *FLP* and *I-SceI* genes. The extrachromosomal target-homologous molecule carrying w^+ marker was produced after FLP-mediated excision and I-SceI–mediated cutting. Homologous recombination of this targeting molecule with the endogenous *dHDAC6* locus produced a tandem duplication which could be screened by w^+ marker. Subsequently, for the reduction of the duplicates (wild-type and mutant forms of *dHDAC6* locus) to a single copy allele, the homologous recombination was stimulated by an I-CreI–generated double-strand break between the duplicated sequences. In the reduction step, w^- flies were selected and further tested for presence of the introduced mutation.

Western Blot and Immunoprecipitation

Adult fly heads with correct genotypes were collected, and proteins were extracted with radioimmunoprecipitation assay buffer (50 mM Tris-HCl, pH 8.0, 150 mM NaCl, 1% NP-40, 0.5% sodium deoxycholate, and 1 mM phenylmethylsulfonyl fluoride) and analyzed by SDS-10% polyacrylamide gel electrophoresis (PAGE). The antibodies used in this experiment are: rabbit anti-dHDAC6 (1:1000; a kind gift from Dr. Hao Li, Novartis Institutes for Biomedical Research, Cambridge, MA; Chen *et al.*, 2008) and rabbit anti-actin (1:1000; Santa Cruz Biotechnology, Santa Cruz, CA). For coimmunoprecipitations, proteins were extracted from 300 brains of *w;TH-GAL4/UAS-α-synuclein* and *w;TH-GAL4/+* of 20-d-old flies and then incubated with agarose beads (Invitrogen, Carlsbad, CA) coupled with A11 antibody (Millipore Bioscience Research Reagents, Temecula, CA) or immunoglobulin G as a control for 8 h at 4°C. After five washes, precipitates were eluted and subjected to SDS-10% PAGE. Rabbit anti-dHDAC6 antibody (1:1000) and anti-α-synuclein antibody (clone 42, 1:1000, BD Biosciences, San Jose, CA) were used for Western blot.

Fractionation Assay

Fractionations of adult fly head lysates were carried out according to a protocol described previously (Chen and Feany, 2005). In brief, 350 heads of correct genotypes with right age were homogenized at 4°C in buffer A (50 mM Tris-HCl, pH 7.5, 1 mM EGTA, 1 mM dithiothreitol with protease inhibitors) and centrifuged at 100,000g for 30 min. The resulting pellets were sequentially extracted by homogenization in Triton X-100 (buffer A containing 1% Triton X-100, 10% sucrose, and 0.5 M sodium chloride), Sarkosyl (50 mM Tris-HCl, pH 7.5, 1% Sarkosyl, and 1 mM EGTA), and urea (50 mM Tris-HCl, pH 7.5, 8 M urea, and 1 mM EGTA) followed by centrifugation at 100,000g for 30 min. Sarkosyl-insoluble and urea-soluble pellets (P) and Tris-soluble supernatants (S) were separated by SDS-PAGE and analyzed by immunoblotting with anti-α-synuclein antibody (clone 42; 1:1000).

Climbing Assay

Climbing assay was performed essentially according to the published protocols (Feany and Bender, 2000; Coulom and Birman, 2004), with some modifications. Twenty adult males were placed into a vertical plastic tube (18 cm in length and 2 cm in diameter). Thirty seconds after being tapped to the bottom of the tube, the number of the flies climbed up over 15 cm was counted. The climbing scores represent the mean percentage of flies that reached the 15-cm line in the total number of flies that were tested. Five trials were performed in each experiment at 1-min intervals, and six experiments were carried out for each genotype. The results were presented as mean ± SEM of the scores obtained in six independent experiments.

Histological Examination of Adult Fly Retinas

For semithin sections, fly heads were fixed with 2.5% glutaraldehyde and postfixed in 1% osmium tetroxide. Then increasing gradient dehydration was performed using ethanol and propylene oxide. Finally, the fixed tissues were embedded in epoxy resin. Tangential retinal sections were performed at a thickness of 1 μm and stained with toluidine blue. Images were obtained with a light microscope (Nikon, Tokyo, Japan) using 60× objective lens.

Immunostaining and Confocal Imaging

Immunostaining of whole-mount adult fly brains were performed as described previously (Wang *et al.*, 2008). In brief, adult fly brains with correct genotypes were dissected in phosphate-buffered saline (PBS) and then fixed with 4% paraformaldehyde for 1 h, followed by washing 3 × 15 min in 0.5% PBT (PBS with 0.5% Triton X-100). The brains were incubated with primary antibody, and then secondary antibody, and finally were mounted in VECTASHIELD (Vector Laboratories, Burlingame, CA). The following primary antibodies were used: rabbit anti-green fluorescent protein (GFP) (1:1000; Invitrogen), mouse monoclonal anti-human α-synuclein (1:10; kindly provided by Dr. Qi-Hong Sun, Beijing Proteome Research Center and Beijing Institute of Radiation Medicine, Beijing, China), and rabbit A11 (1:100; Millipore Bioscience Research Reagents). The fluorescent secondary antibodies (1:100; Jackson ImmunoResearch Laboratories, West Grove, PA) were selected accordingly to visualize the protein expression patterns in the brain. Confocal images were obtained on an SP5 microscope (Leica, Nussloch, Germany).

Automated Quantification of Inclusions and Oligomers

The automated quantification was performed by analyzing the individual confocal Z-series with the image processing software ImageJ version 1.37 (National Institutes of Health, Bethesda, MD) as described previously (Botella *et al.*, 2008). After background correction and color depth reduction to 8 bits, the detection threshold was set to no <20. Then, automated quantification was performed with the "analyze particles" function with a minimal size of 1 pixel, and the particles were scored automatically. For inclusion number, the automatic particle counts were analyzed. For inclusion size analysis, we defined large inclusions as >1 μm at diameter and assessed their number. For oligomer amount quantification, the pixel area of A11-positive signals was recorded from the dorsal regions of the brain as shown in Figure 7.

RESULTS

Generation and Characterization of the dHDAC6 Mutants

HDAC6 has been shown to function in the clearance of misfolded protein in mammalian cell lines (Boyault *et al.*, 2007a). We used loss-of-function study for *dHDAC6*, the *Drosophila* homologue of mammalian *HDAC6*, to investigate the role of dHDAC6 in *Drosophila* PD model. In this aim, we generated null allele of dHDAC6 (*dHDAC6^{KO}*) by using targeted mutagenesis (Rong and Golic, 2000). A translation start codon mutation and a frame shift were introduced in the *dHDAC6* open reading frame (Figure 1, A and B). Western blot result confirmed that no dHDAC6 protein was produced in homozygous *dHDAC6^{KO}* flies (Figure 1C). The rescue experiments validated the specificity of the knockout mutation (Supplemental Figure S1; data not shown). The mutant flies were viable and fertile and exhibited no obvious
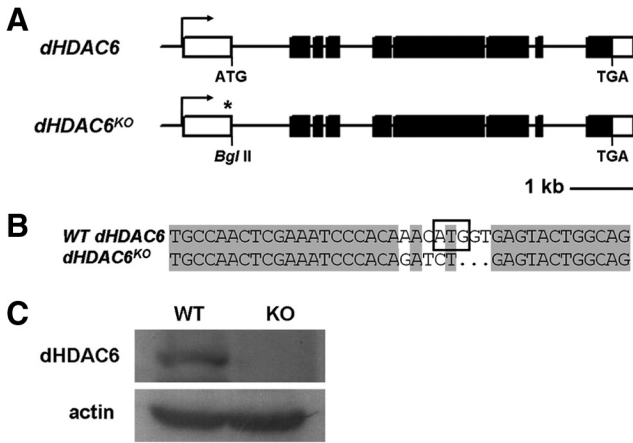
A

B

WT dHDAC6 TGCCAACTCGAAATCCCACAAACATGGTGAGTACTGGCAG
dHDAC6^KO TGCCAACTCGAAATCCCACAGATCT . . . GAGTACTGGCAG

C

Figure 1. Characterization of the *dHDAC6^KO* mutant. (A) Genomic organization of the *Drosophila dHDAC6* locus and the mutant allele of *dHDAC6*. Asterisk indicates the mutation of the ATG start codon. Filled bars are the coding regions; open bars are the untranslated regulatory regions. (B) Part of the *dHDAC6^KO* mutant genomic sequence that contains point mutation and frame shift at the *dHDAC6* translation start codon. The boxed sequence is *dHDAC6* start codon in the wild-type gene. (C) dHDAC6 protein is absent in the *dHDAC6* mutant flies as shown by Western blot. Protein extracts from wild-type (WT) and *dHDAC6* knockout (KO) flies were blotted with anti-HDAC6 and anti-actin antibodies. Actin was used as a loading control.

morphological abnormalities under normal culture conditions. With oxidative or heat stress *dHDAC6^KO* flies did not show any notable difference from wild-type animals (Supplemental Figure S2). These results demonstrate that dHDAC6 is dispensable for viability, fertility and resistance to heat and oxidative stress in *Drosophila*. The viability of the homozygous *dHDAC6^KO* flies makes it genetically tractable to ablate dHDAC6 in α-synuclein-induced PD adult flies in the subsequent study.

dHDAC6 Mutation Exacerbates Neurodegeneration in the Drosophila PD Model

The expression of human α-synuclein in the *Drosophila* nervous system stimulates the loss of tyrosine hydroxylase (TH)-positive dopaminergic neurons (Feany and Bender, 2000; Auluck *et al.*, 2002). To determine whether dHDAC6 participates in this process, we used the GAL4/UAS system to express α-synuclein specifically in the DA neurons of *dHDAC6^KO* (*dHDAC6^KO*; *α-syn*) and wild-type (*α-syn*) flies. Because the expression pattern of the driver-*TH-GAL4* has been shown to be specifically associated with the DA system (Friggi-Grelin *et al.*, 2003; this study; and Supplemental Figure S3), we used *TH-GAL4* to drive the expression of *UAS-mCD8::GFP* to visualize and quantitatively measure the DA neurons in the adult fly brain.

Four *Drosophila* strains of *dHDAC6^KO*, *α-syn*, *dHDAC6^KO*; *α-syn*, and the wild type as a control were examined for DA neurons. No significant difference in the number of DA neurons was detected in the 1-d-old flies of these strains (Figure 2, A and D) or in the 10- and 20-d-old wild-type and *dHDAC6^KO* flies (Figure 2, B and C and E and F). Significant loss of DA neurons was observed not only in the dorsomedial (DM) but also in the posteriomedial (PM) and the dorsolateral (DL)₁ clusters of the *α-syn* flies at the age of 20 d (Figure 2, C and F), whereas there was no distinguishable loss of DA neurons in that of 10-d-old *α-syn* flies (Figure 2,

B and E). The abrogation of dHDAC6 enhanced the α-synuclein-induced DA neuron loss phenotype, especially in the DM and DL₁ clusters (Figure 2, B and C and E and F). In the *dHDAC6^KO*; *α-syn* flies, the neuron degeneration phenotype appeared at the age of 10 d, which is earlier than in *α-syn* flies, and the phenotype worsened with age. The total DA neuron number in DM, PM, and DL₁ clusters of *dHDAC6^KO*; *α-syn* flies decreased ∼29% at 10 d of age and ∼36% at 20 d compared with that in 1-d-old wild-type flies, whereas the total DA neuron number in the *α-syn* flies only declined ∼5% at 10 d of age and ∼11% at 20 d of age. Quantitative analysis of the total number of DA neurons in DM, PM, and DL₁ clusters revealed that ectopic α-synuclein expression driven by *TH-GAL4* resulted in progressive DA neuron loss, and the absence of dHDAC6 aggravated this α-synuclein-induced DA neuron loss phenotype (Figure 2G). Together, these results demonstrate that the loss of dHDAC6 enhances the degeneration of DA neurons caused by overexpression of α-synuclein.

To gain more insight into the impact of dHDAC6 on α-synuclein–induced neurodegeneration, additional neural context was examined. We used *GMR-GAL4* to express α-synuclein in the eyes. The photoreceptor cells, neuronal cells in the ommatidia, are prone to the effect of neurotoxicity (Feany and Bender, 2000). The *GMR-GAL4/+* flies did not show any detectable morphological defects in the eyes. Retinal sections reveal that the inner structure of eyes of these flies was intact and normal, with seven photoreceptor cells properly arranged in a regular pattern (Figure 3, A and B). However, the *α-syn* flies between the age of 20 and 30 d exhibited neurodegenerative phenotype in the eyes, with less photoreceptor cells and retinal distortion (Figure 3). This age-dependant phenotype was worsened in *dHDAC6* mutant flies. The 20-d-old *dHDAC6^KO*; *α-syn* flies exhibited fewer photoreceptor cells in a severely disrupted internal eye structure as compared with *α-syn* flies (Figure 3, A and C). In *dHDAC6^KO* flies, the eye morphology and inner retinal structure are comparable to *GMR-GAL4/+* control flies (Figure 3, A and C). These observations further support that dHDAC6 plays a protective role in coping with the α-synuclein neurotoxicity.

Next, we sought to examine whether increased dose of dHDAC6 can suppress α-synuclein neurotoxicity. To this end, a copy of *UAS-dHDAC6* transgene was introduced into the *α-syn* flies and the analysis was carried out at 30 d after eclosion. Overexpression of dHDAC6 restored ommatidia integrity, especially the number of photoreceptor cells caused by α-synuclein overexpression, suggesting that dHDAC6 can alleviate the α-synuclein toxicity (Figure 3, B, D, and E). Furthermore, the role of dHDAC6 that overcomes the α-synuclein toxicity is manifested by the observation that overexpression of dHDAC6 rescued the DA neuron loss phenotype (Supplemental Figure S4). Collectively, both loss-of-function and gain-of-function data support the conclusion that dHDAC6 protects neurons from α-synuclein–derived toxicity.

dHDAC6 Mutation Promotes α-Synuclein–induced Locomotor Dysfunction

In the fly PD model, progressive DA neuron degeneration was reported to be accompanied with an age-dependent locomotor dysfunction (Feany and Bender, 2000). We used climbing assay (Coulom and Birman, 2004) to test the impacts of dHDAC6 on the locomotion ability of the modeled PD flies (*dHDAC6^KO*; *α-syn* flies vs. *α-syn* flies) at 5-d intervals for a period of 20 d (Figure 4). Compared with the wild-type control, both of the transgenic lines had no detect-
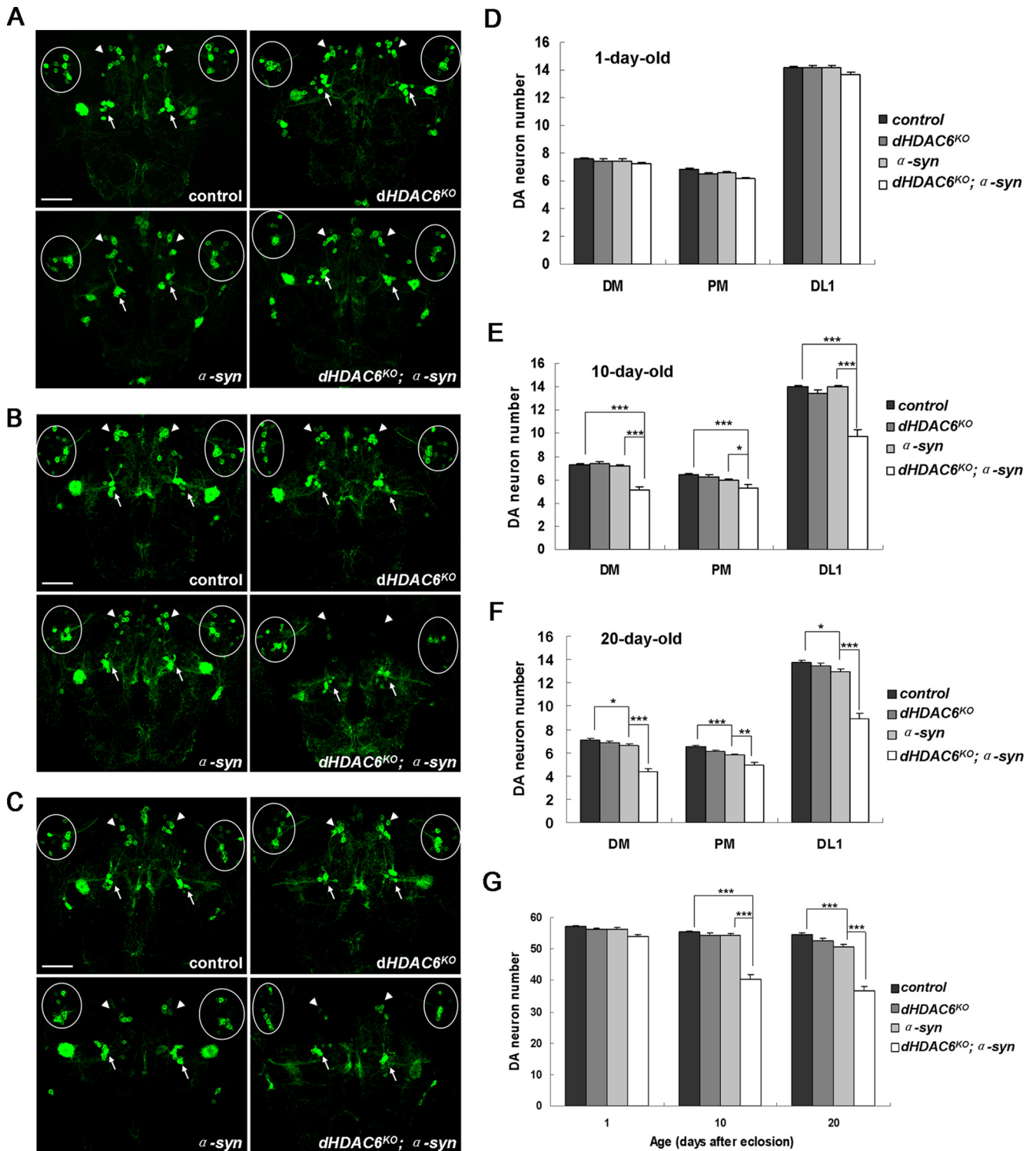
Figure 2. *dHDAC6^KO* promotes α-synuclein–induced dopaminergic neuron loss. Confocal images of dopaminergic neurons in DM, PM, and DL$_1$ regions immunostained with anti-GFP antibody on 1-d-old (A), 10-d-old (B), and 20-d-old (C) fly brains, respectively, are shown, with arrows for PM and arrowheads for DM clusters and circles for DL$_1$ clusters. (D–F) Quantitative graphs are shown corresponding to confocal images of 1-d-old, 10-d-old, and 20-d-old fly brains, respectively. (G) Graphs showing total numbers of dopaminergic neurons in the DM, PM, and DL$_1$ clusters of different genotypes as indicated at 1 d, 10 d, 20 d. Data were analyzed by Student's *t* test and presented as mean ± SEM (n = 20~40) with * for p < 0.05, ** for p < 0.01, and *** for p < 0.001. Bar, 50 μm. Genotypes: *control* flies are *w; UAS-mCD8::GFP/+; TH-GAL4/+. dHDAC6^KO* flies are *w, dHDAC6^KO; UAS-mCD8::GFP/+; TH-GAL4/+. α-syn* flies are *w; UAS-mCD8::GFP/+; TH-GAL4, UAS-α-synuclein/+. dHDAC6^KO; α-syn* flies are *w, dHDAC6^KO; UAS-mCD8::GFP/+; TH-GAL4, UAS-α-synuclein/+.*
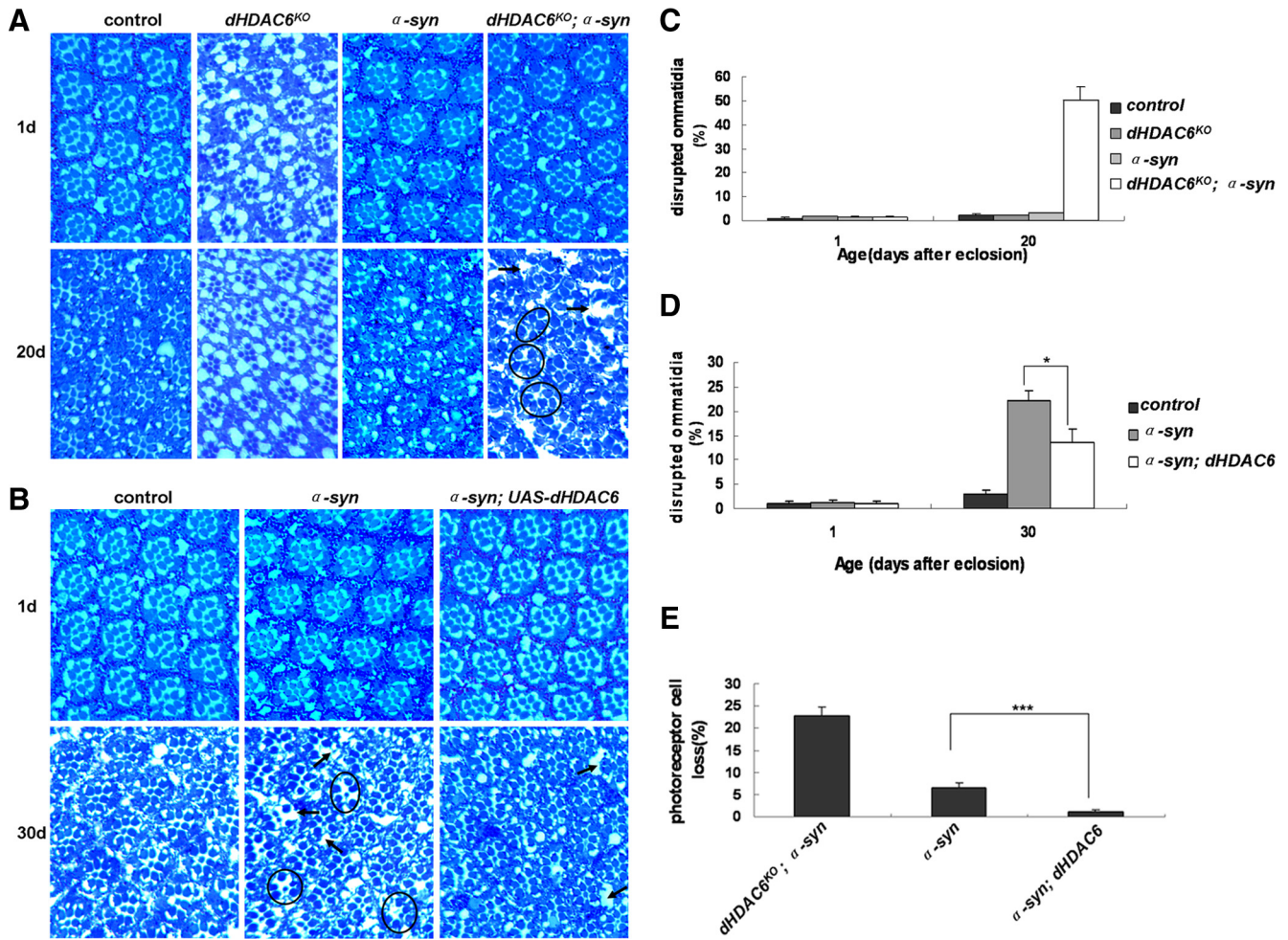
Figure 3. Loss of dHDAC6 exacerbates retinal degeneration in α-synuclein–expressing eyes and overexpression of dHDAC6 counteracts the α-synuclein neurotoxicity. Semithin sections of retina showing inner retinal structures of 1-d-old (A and B, top), 20-d-old (A, bottom), and 30-d-old (B, bottom) flies. Arrows indicate outer ring disintegration of the ommatidia. Circles indicate ommatidia with loss of photoreceptor cells. (C) Quantification of disrupted ommatidia in *control*, *dHDAC6-L^KO*, *α-syn* and *dHDAC6-L^KO;α-syn* flies at 1 and 20 d after eclosion. (D) Quantification of disrupted ommatidia in *control*, *α-syn*, and *α-syn;dHDAC6* flies at 1 and 30 d. (E) Quantification of ommatidia with photoreceptor cell loss in 20-d-old *dHDAC6^KO;α-syn* flies, 30-d-old *α-syn* flies, and *α-syn;dHDAC6* flies. Note that the retinal pattern and seven photoreceptor cells were normal in *GMR-GAL4* control and *dHDAC6-L^KO* flies. No discernible photoreceptor loss was detected in 1-d-old and 20-d-old *α-syn* flies. Data were analyzed by Student's *t* test and presented as mean ± SEM (n > 5) with *p < 0.05, **p < 0.01, and ***p < 0.001. Genotypes: *control* flies are *w; GMR-GAL4/+*. *dHDAC6-L^KO* flies are *w, dHDAC6-L^KO*. *α-syn* flies are *w; GMR-GAL4/+; UAS-α-synuclein/+*. *dHDAC6-L^KO; α-syn* flies are *w, dHDAC6-L^KO; GMR-GAL4/+; UAS-α-synuclein/+*. *α-syn; dHDAC6* flies are *w; GMR-GAL4/+; UAS-α-synuclein/UAS-dHDAC6*.

able climbing defect in their early ages. At the age of 10 d, the climbing ability of *dHDAC6^KO; α-syn* flies but not *α-syn*

flies was significantly impaired (Figure 4), and progressively deteriorated in an age-dependent manner. In contrast, no-
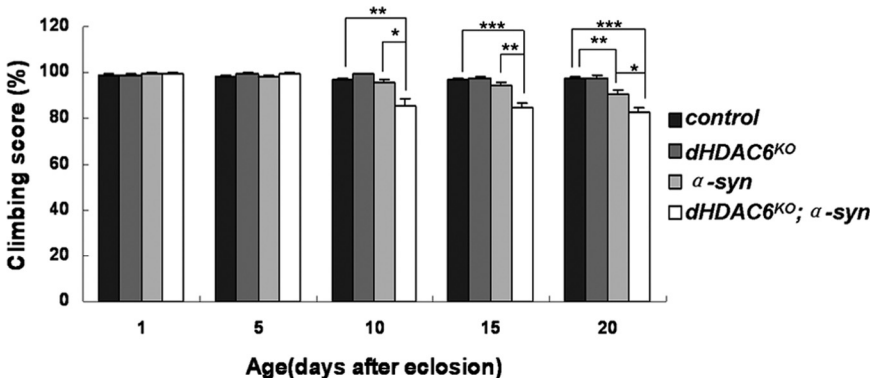

Figure 4. *dHDAC6^KO* enhances the climbing defects caused by α-synuclein overexpression. Bars show the percentage of the flies that climbed to reach 15 cm in 30 s at different ages with the genotypes as indicated. Data were analyzed by Student's *t* test and presented as mean ± SEM (n = 120) with *p < 0.05, **p < 0.01, and ***p < 0.001. Genotypes: *control* flies are *w; TH-GAL4/+*. *dHDAC6-L^KO* flies are *w, dHDAC6-L^KO; TH-GAL4/+*. *α-syn* flies are *w; TH-GAL4/UAS-α-synuclein*. *dHDAC6^KO; α-syn* flies are *w, dHDAC6^KO; TH-GAL4/UAS-α-synuclein*.
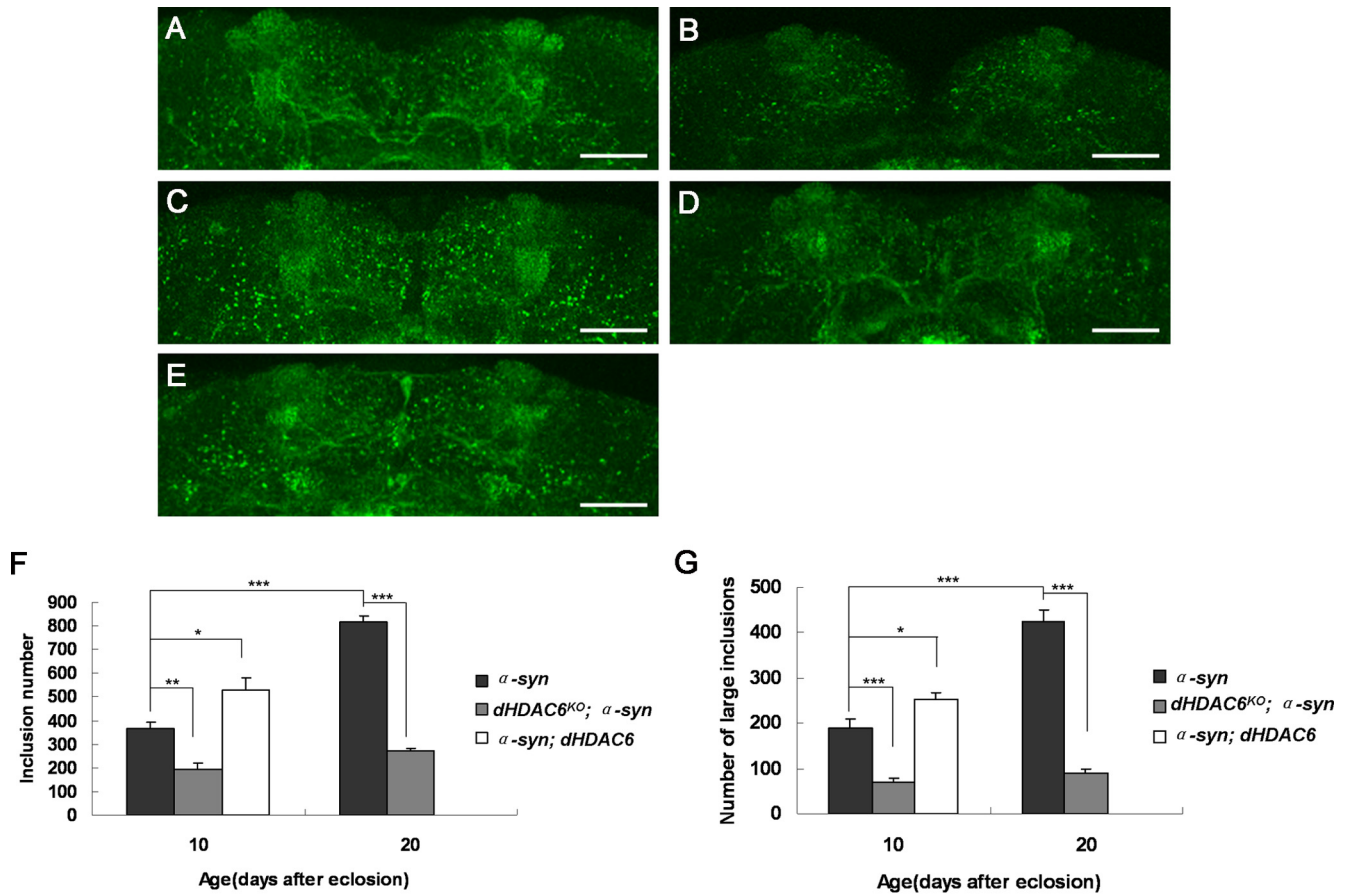
Figure 5. The amount of LB-like inclusion decreases in *dHDAC6^{KO}* flies with α-synuclein overexpression. LB-like inclusions in the DM region of *α-syn* (A and C) and *dHDAC6^{KO}*; *α-syn* flies (B and D) at 10 d (A and B) and 20 d (C and D) were labeled by whole-mount immunostaining with anti-α-synuclein antibody. (E) Inclusions when *UAS-dHDAC6* transgene is expressed in *α-syn* flies at 10 d old. Bar, 40 μm. (F and G) Quantification of the numbers of total inclusions (F) and large inclusions that are >1 μm (G) at 10 d old and 20 d old with the genotypes as indicated on the right. Data were analyzed by Student's *t* test and presented as mean ± SEM (n > 5) with *p < 0.05, **p < 0.01, and ***p < 0.001. Genotypes: flies in A and C are *w; TH-GAL4/UAS-α-synuclein*. Flies in B and D are *w, dHDAC6^{KO}; TH-GAL4/UAS-α-synuclein*. Fly in E is *w; UAS-dHDAC6/+; TH-GAL4, UAS-α-synuclein/+*.

ticeable climbing defects in *α-syn* flies did not appear until the age of 20 d in our study. Furthermore, the climbing defects in 20-d-old *dHDAC6^{KO}*; *α-syn* flies were also more pronounced than in *α-syn* flies. It also should be mentioned that there was no locomotion defect in *dHDAC6^{KO}* flies at all five individual surveyed ages (Figure 4). Together, *dHDAC6* mutation enhances the locomotor defects in PD modeled flies. Considering the other observations that 1) a sudden loss of DA neurons happens at ~10th day after eclosion (Figure 2, B and E); and 2) a sharp decrease of survival rate occurs at the age of 10 d (Supplemental Figure S5) in *dHDAC6^{KO}*; *α-syn* flies, we suggest that the enhancement of locomotor defects and life span shortening by *dHDAC6* mutation is associated with DA neuron degeneration in PD modeled flies. We propose that 10 d after eclosion may be a "checkpoint" for the fly parkinsonism. These three lines of evidence (neurodegeneration, climbing ability, and longevity) demonstrate that dHDAC6 suppresses the α-synuclein-induced pathological progression in fly PD model.

dHDAC6 Is Essential for the Formation of α-Synuclein–positive Inclusions in the Drosophila PD Model

PD is usually associated with the formation of LBs (Lang and Lozano, 1998). LB-like inclusions containing α-synuclein have been found in flies that ectopically express α-synuclein (Feany and Bender, 2000). To evaluate the biological importance of dHDAC6 on LB-like inclusion formation, α-synuclein antibody was used to visualize the density of this property on whole-mount fly brains.

Aggregates detectable with 20× magnification objective were considered as LB-like inclusions (McLean *et al.*, 2002). In 1-d-old *α-syn* fly brains, the immunostaining of α-synuclein showed diffuse pattern (data not shown), which is similar to the case of young fly brains reported previously (Feany and Bender, 2000). The α-synuclein-positive inclusions in the neuropil adjacent to the DM region of the brains were clearly observed in 10- and 20-d-old *α-syn* flies (Figure 5, A and C). The number and the size of inclusions in *α-syn* flies were gradually increased along with age (Figure 5, F and G). However, fewer LB-like inclusions were present in the same region of *dHDAC6^{KO}*; *α-syn* flies at 20 d of age (Figure 5, D and F), and no such inclusion was detectable in 10-d-old flies (Figure 5, B and F). The *α-syn*, *dHDAC6^{KO}*; *α-syn* and *α-syn; UAS-dHDAC6* flies have comparable amounts of total α-synuclein, arguing against the possibility that the observed effects are a consequence of reduced α-synuclein expression level (Figure 6B). To confirm the immunostaining results, we took advantage of sarkosyl-
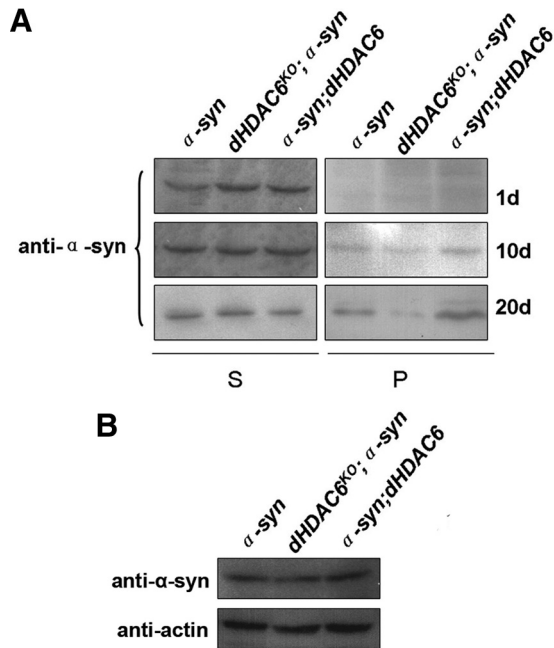
A

B

Figure 6. dHDAC6 positively regulates the accumulation of insoluble α-synuclein. (A) Immunoblots detecting α-synuclein from the fractions (see *Materials and Methods* for details of fractionation) of Tris-soluble supernatant (S) and Sarkosyl-insoluble/urea-soluble pellets (P). The flies were 1 d old, 10 d old, and 20 d old, respectively. (B) Western blot of α-synuclein from the heads of 1-d-old flies that express α-synuclein under the control of *TH-GAL4* in the backgrounds of *wild-type*, *dHDAC6^{KO}*, and dHDAC6 overexpression, as indicated on the top. The membrane was first probed with α-synuclein antibody and then stripped before immunoblotted with anti-actin that serves as a loading control. Genotypes: *α-syn* flies are *w; TH-GAL4/UAS-α-synuclein*. *dHDAC6^{KO}; α-syn* flies are *w, dHDAC6^{KO}; TH-GAL4/UAS-α-synuclein*. *α-syn; dHDAC6* flies are *w; UAS-dHDAC6/+; TH-GAL4, UAS-α-synuclein/+*.

insoluble, urea-soluble feature of inclusions (Chen and Feany, 2005), and performed fractionations of fly head lysates. Our results show a reduced amount of sarkosyl-insoluble and urea-soluble pellets in *α-syn* flies lacking *dHDAC6* (Figure 6A). These data demonstrate that dHDAC6 plays a crucial role in the formation of LB-like inclusions in *α-synuclein–*expressing flies. It also indicates that the inclusions are cytoprotective in the process of neurodegeneration.

To further assess the dHDAC6 function in the formation of LB-like inclusions, we generated transgenic flies that conditionally express dHDAC6 by using the GAL4/UAS system. When α-synuclein and dHDAC6 were coexpressed in DA neurons, the amount of inclusions was substantially elevated compared with the flies that expressed α-synuclein solely (Figure 5, A, E, and F). Overexpression of dHDAC6 also led to an increase in sarkosyl-insoluble and urea-soluble pellets in fractionation experiments (Figure 6A). This observation suggests that the dHDAC6 dosage directly controls the formation of inclusions, further supporting the notion that dHDAC6 facilitates inclusion formation to attenuate α-synuclein–induced toxicity.

dHDAC6 Suppresses Oligomer Accumulation through Physical Interaction in the Drosophila PD Model

In vivo and in vitro studies have shown that α-synuclein monomers can be sequentially assembled into several conformations, including oligomers, protofibrils, fibrils, and

tightly packed form in LBs (Conway *et al.*, 1998; Periquet *et al.*, 2007). The oligomeric or protofibrillar forms of α-synuclein have been suggested to be more toxic than the mature fibril forms (Lashuel *et al.*, 2002; Sharon *et al.*, 2003). To further ascertain that dHDAC6 functions in protecting neurons from α-synuclein toxicity through reducing the toxic forms of α-synuclein, we examined oligomer accumulation in α-synuclein expressing flies in the presence and absence of dHDAC6. We probed oligomers with A11 antibody that recognizes a structure-specific epitope of amyloidogenic proteins and reacts with all the soluble oligomeric aggregates, including oligomers and protofibrils (Kayed *et al.*, 2003). The specificity of A11 to oligomeric α-synuclein has been reported in the previous studies (Kayed *et al.*, 2003; Kim *et al.*, 2009; Yu *et al.*, 2009) and shown in this study (Supplemental Figure S8). In wild-type flies at different ages, no oligomer in the dorsal region of the brain was detected by A11 antibody (Figure 7F). In both transgenic flies (*α-syn* and *dHDAC6^{KO}; α-syn*) at 1 d old, no oligomer-specific deposit was found in the dorsal region of the brain either (data not shown). Oligomer-specific immunoreactivity was detected in 20-d-old *α-syn* flies (Figure 7C) but not of 10-d-old *α-syn* flies (Figure 7A). Compared with *α-syn* flies of the same age, the oligomer staining in *dHDAC6^{KO}; α-syn* flies were considerably increased (Figure 7, B, D, and G). Conversely, overexpression of dHDAC6 led to detectable reduction of the oligomers (Figure 7, E and G). These results indicate that DA neuron loss is correlated to the increased level of α-synuclein oligomers (Figures 2 and 7), and the oligomers are thus very likely toxic to DA neurons. In addition, neither DA neuron loss (Figure 2, A and D) nor α-synuclein aggregates (data not shown) were observed in 1-d-old *α-syn* flies, suggesting that α-synuclein monomers do not induce DA neuron loss. These data indicate that dHDAC6 protects cells from α-synuclein toxicity by decreasing the amount of oligomers.

To determine whether dHDAC6 physically interacts with oligomers, we performed coimmunoprecipitation assay. Because the A11 antibody recognizes the structure that is vulnerable to SDS (Karpinar *et al.*, 2009), we used this antibody for immunoprecipitation to determine whether dHDAC6 could be coimmunoprecipitated instead of performing the reverse immunoprecipitation. The extracts were prepared from the heads of 20-d-old *α-syn* flies and flies that do not express α-synuclein. The physical interaction between dHDAC6 and α-synuclein oligomer was detected in the coimmunoprecipitation experiment as shown in Figure 8A. Immunoblotting results with α-synuclein antibody validated the ability of A11 to immunoprecipitate oligomeric α-synuclein aggregates but not monomeric α-synuclein (Figure 8A and Supplemental Figure S8). No dHDAC6 was precipitated in the flies without α-synuclein (Figure 8B). These results further strengthen the view that dHDAC6 regulates the amount of α-synuclein oligomers by physically interacting with each other in vivo.

DISCUSSION

In this study, we provide evidence for the first time that dHDAC6 protects DA neurons from α-synuclein toxicity by promoting inclusion formation and decreasing the amount of α-synuclein oligomers in the *Drosophila* PD model. We show that mutation of *dHDAC6* notably affects the key features of PD in the α-synuclein modeled flies, namely selective loss of DA neurons, formation of α-synuclein-containing inclusions in the brain, decrease of locomotion ability, and shortening of life span. In addition, our genetic experiments show that dHDAC6 also functions to prevent the
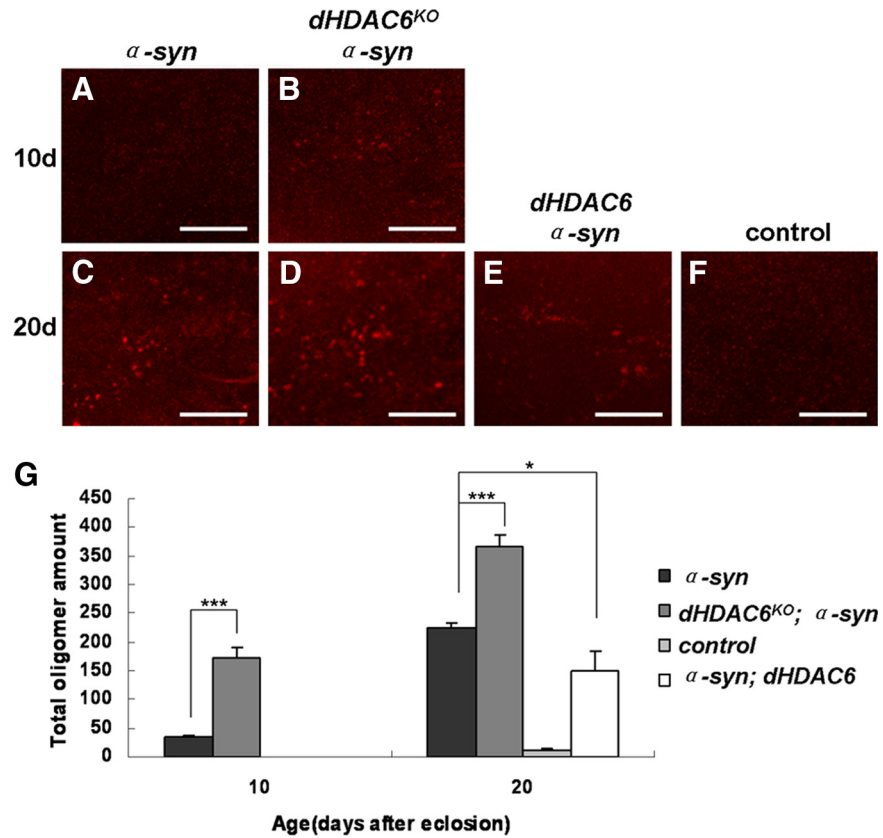
Figure 7. Oligomers accumulate in *dHDAC6^{KO}* fly brains with α-synuclein overexpression. Oligomers in the dorsal brain area of *α-syn* flies (A and C) and *dHDAC6^{KO}*; *α-syn* flies (B and D) at 10 (A and B) and 20 d (C and D) were visualized in red by oligomer-specific antibody A11. (E) *α-syn* flies at 20 d with dHDAC6 overexpression showing A11 signals. (F) Wild-type control flies at 20 d probed with A11. Bar, 20 μm. (G) Quantitative graphs showing the total A11-positive signals (oligomers) in the dorsal region of the brain as shown in A–F. Data were analyzed by Student's *t* test and presented as mean ± SEM (n > 5) with *p < 0.05, **p < 0.01, and ***p < 0.001. Genotypes: *α-syn* flies are *w; TH-GAL4/UAS-α-synuclein*. *dHDAC6^{KO}*; *α-syn* flies are *w, dHDAC6^{KO}; TH-GAL4/UAS-α-synuclein*. *Control* flies are *TH-GAL4/+*.

toxicity induced by overexpression of glutamine expanded human Spinocerebellar ataxia type 3 (SCA3) which is also known as Machado-Joseph disease (MJD) (Supplemental Figure S6). Furthermore, as shown in Supplemental Figure S1 mutation of *dHDAC6* leads to a more severe rough eye phenotype characterizing impaired ubiquitin proteasome system (UPS) (Belote and Fortier, 2002), suggesting that *dHDAC6* may play a compensatory role in the impaired UPS. Together, these lines of evidence indicate multiple roles of dHDAC6 in protein quality control machinery in vivo.

In vitro studies in our laboratory (Huang *et al.*, 2006) and other laboratories (Cookson, 2005) show that α-synuclein exists as soluble and unfolded monomers under physiolog-

ical conditions, but with a tendency to form fibrils under certain conditions through gradual polymerization to oligomers/protofibrils and finally to inclusions/fibrils. Although LBs are present in most of the clinically diagnosed PD patients, not every factor involved in this disorder has clear relationship with LB inclusion formation (Cookson *et al.*, 2008). In this study, we demonstrated alteration of dHDAC6 dose remarkably affects the density of α-synuclein inclusions, suggesting that dHDAC6 is an integral factor in the process of inclusion formation in vivo. Outeiro *et al.* (2007) reported that Sirtuin 2 regulates the inclusion morphology in human H4 neuroglioma cells. Chen and Feany reported that blocking phosphorylation at Ser129 of α-synuclein substantially increased inclusion formation in *Drosophila* PD model (Chen and Feany, 2005). Mutation of Synphilin-1 was reported to be able to reduce the formation of α-synuclein inclusions in human neuroblastoma SH-SY5Y cells (Marx *et al.*, 2003). It seems that the formation of inclusions is a complex issue hardly dominated by a single gene. We used genetic approaches to test for potential cooperators of dHDAC6 in this event and found that transgenic expression of Hsp70 can rescue, at least partially, the inclusion formation defect caused by abrogation of dHDAC6 (Supplemental Figure S7). This suggests that Hsp70 may be partially epistatic to dHDAC6, however, the possibility that they function in parallel in large inclusion body formation is not excluded by this experiment. Because the inclusions in the brains of the *dHDAC-L^{KO}*; *α-syn* line are not abolished (Figure 5, B and D), we speculate that besides the dHDAC6-related pathway, other parallel pathway(s) also may be implicated in α-synuclein inclusion formation. Further experiments are required to elucidate the mechanism of formation and regulation of inclusions.
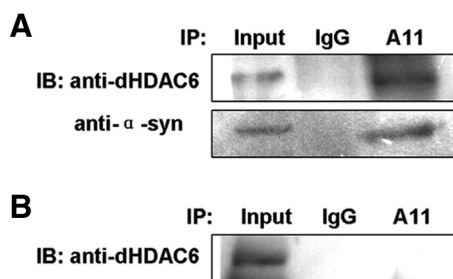

Figure 8. dHDAC6 physically interacts with oligomeric α-synuclein in *Drosophila*. Protein extracts for immunoprecipitation were prepared from the brains of 20-d-old flies: *w; TH-GAL4/UAS-α-synuclein* (A, with α-synuclein expression) and *w; TH-GAL4/+* (B, without α-synuclein expression). The SDS-10% PAGE of the coimmunoprecipitation samples was immunoblotted with anti-dHDAC6 (A, top; and B) or anti-α-synuclein antibody (A, bottom). Input: 20% of the extracts that were used for immunoprecipitation.

Oligomer is a conformational intermediate of α-synuclein aggregates. Our data have shown that abrogation of dHDAC6 results in increase of oligomers. Kawaguchi *et al.*, (2003) demonstrate the association of HDAC6 with ubiquitinated misfolded proteins to form aggresomes in cell culture. Our coimmunoprecipitation assays show that HDAC6 associates with oligomeric α-synuclein, suggesting a role of dHDAC6 in the dynamics of α-synuclein oligomers. We propose that dHDAC6 binds to and promotes the toxic oligomers to change their conformations and form protective inclusions. However, the possibility that dHDAC6 may inhibit the oligomerization of α-synuclein cannot be excluded. A few factors have been identified to contribute to oligomerization with biochemical pathology methods. Polyunsaturated fatty acids increase oligomerization, whereas saturated fatty acids and rifampicin show opposite effects (Sharon *et al.*, 2003; Xu *et al.*, 2007). G protein-coupled receptor kinase (GRK)5 and Hsp70 have been characterized to be related to α-synuclein oligomerization. GRK5 promotes, whereas Hsp70 inhibits, oligomer formation (Arawaka *et al.*, 2006; Outeiro *et al.*, 2008). Given the functional relationship between HDAC6 and Hsp70 (Boyault *et al.*, 2007b), a potential cooperative role of these two proteins in the oligomerization process may emerge.

The problem of which form/s of α-synuclein are toxic has been controversial. Inclusions used to be widely considered as a toxic component (Conway *et al.*, 1998; Tu *et al.*, 1998), whereas, increasing evidence suggests its role as a successful defense by lowering the concentration of toxic forms (Taylor *et al.*, 2003; Arrasate *et al.*, 2004). We monitored neuron cell mortality and retinal structure to assess the toxicity of different conformations of α-synuclein. Comparison of the neuron cell number, inclusion population and oligomer abundance between young flies and aged flies makes us to draw three sets of conclusions. First, monomeric α-synuclein is not toxic for neuron cells. Second, oligomers are toxic to the neuron cells. Finally, inclusions are cytoprotective form and protect neurons from α-synuclein toxicity. The three features, fewer neurons, fewer inclusions, and increased oligomers in aged *dHDAC6^{KO}; α-syn* flies recapitulate the intrinsic essence of PD symptom progression. Our results provide the first insight into the in vivo evaluation of the toxicity of different α-synuclein conformation and build avenues for putative targets for dealing with α-synuclein toxicity.

Functional studies of the mechanism behind PD pathogenesis are required for therapeutic drug design. Our findings suggest that formation of inclusions or elimination of soluble α-synuclein oligomers, a process that involves dHDAC6, represents potential preventative targets. If this mechanism is conserved in humans, HDAC6 may offer a promising target for clinical therapy of PD patients through the up-regulation or enhancement of its activity.

ACKNOWLEDGMENTS

REFERENCES

Arawaka, S., *et al.* (2006). The role of G-protein-coupled receptor kinase 5 in pathogenesis of sporadic Parkinson's disease. J. Neurosci. *26*, 9227–9238.

Arrasate, M., Mitra, S., Schweitzer, E. S., Segal, M. R., and Finkbeiner, S. (2004). Inclusion body formation reduces levels of mutant huntingtin and the risk of neuronal death. Nature *431*, 805–810.

Auluck, P. K., Chan, H. Y., Trojanowski, J. Q., Lee, V. M., and Bonini, N. M. (2002). Chaperone suppression of alpha-synuclein toxicity in a *Drosophila* model for Parkinson's disease. Science *295*, 865–868.

Belote, J. M., and Fortier, E. (2002). Targeted expression of dominant negative proteasome mutants in *Drosophila melanogaster*. Genesis *34*, 80–82.

Botella, J. A., Bayersdorfer, F., and Schneuwly, S. (2008). Superoxide dismutase overexpression protects dopaminergic neurons in a *Drosophila* model of Parkinson's disease. Neurobiol. Dis. *30*, 65–73.

Boyault, C., Gilquin, B., Zhang, Y., Rybin, V., Garman, E., Meyer-Klaucke, W., Matthias, P., Muller, C. W., and Khochbin, S. (2006). HDAC6–p97/VCP controlled polyubiquitin chain turnover. EMBO J. *25*, 3357–3366.

Boyault, C., Sadoul, K., Pabion, M., and Khochbin, S. (2007a). HDAC6, at the crossroads between cytoskeleton and cell signaling by acetylation and ubiquitination. Oncogene *26*, 5468–5476.

Boyault, C., *et al.* (2007b). HDAC6 controls major cell response pathways to cytotoxic accumulation of protein aggregates. Genes Dev. *21*, 2172–2181.

Chen, J., Shi, X., Padmanabhan, R., Wang, Q., Wu, Z., Stevenson, S. C., Hild, M., Garza, D., and Li, H. (2008). Identification of novel modulators of mitochondrial function by a genome-wide RNAi screen in *Drosophila melanogaster*. Genome Res. *18*, 123–136.

Chen, L., and Feany, M. B. (2005). alpha-Synuclein phosphorylation controls neurotoxicity and inclusion formation in a *Drosophila* model of Parkinson disease. Nat. Neurosci. *8*, 657–663.

Conway, K. A., Harper, J. D., and Lansbury, P. T. (1998). Accelerated in vitro fibril formation by a mutant alpha-synuclein linked to early-onset Parkinson disease. Nat. Med. *4*, 1318–1320.

Cookson, M. R. (2005). The biochemistry of Parkinson's disease. Annu. Rev. Biochem. *74*, 29–52.

Cookson, M. R., Hardy, J., and Lewis, P. A. (2008). Genetic neuropathology of Parkinson's disease. Int. J. Clin. Exp. Pathol. *1*, 217–231.

Coulom, H., and Birman, S. (2004). Chronic exposure to rotenone models sporadic Parkinson's disease in *Drosophila melanogaster*. J. Neurosci. *24*, 10993–10998.

Egli, D., *et al.* (2006). A family knockout of all four *Drosophila* metallothioneins reveals a central role in copper homeostasis and detoxification. Mol. Cell. Biol. *26*, 2286–2296.

Feany, M. B., and Bender, W. W. (2000). A *Drosophila* model of Parkinson's disease. Nature *404*, 394–398.

Friggi-Grelin, F., Coulom, H., Meller, M., Gomez, D., Hirsh, J., and Birman, S. (2003). Targeted gene expression in *Drosophila* dopaminergic cells using regulatory sequences from tyrosine hydroxylase. J. Neurobiol. *54*, 618–627.

Huang, C., Cheng, H., Hao, S., Zhou, H., Zhang, X., Gao, J., Sun, Q. H., Hu, H., and Wang, C. C. (2006). Heat shock protein 70 inhibits alpha-synuclein fibril formation via interactions with diverse intermediates. J. Mol. Biol. *364*, 323–336.

Jankovic, J. (2008). Parkinson's disease: clinical features and diagnosis. J. Neurol. Neurosurg. Psychiatry *79*, 368–376.

Karpinar, D. P., *et al.* (2009). Pre-fibrillar alpha-synuclein variants with impaired beta-structure increase neurotoxicity in Parkinson's disease models. EMBO J. *28*, 3256–3268.

Kawaguchi, Y., Kovacs, J. J., McLaurin, A., Vance, J. M., Ito, A., and Yao, T. P. (2003). The deacetylase HDAC6 regulates aggresome formation and cell viability in response to misfolded protein stress. Cell *115*, 727–738.

Kayed, R., Head, E., Thompson, J. L., McIntire, T. M., Milton, S. C., Cotman, C. W., and Glabe, C. G. (2003). Common structure of soluble amyloid oligomers implies common mechanism of pathogenesis. Science *300*, 486–489.

Kim, H. Y., *et al.* (2009). Structural properties of pore-forming oligomers of alpha-synuclein. J. Am. Chem. Soc. *131*, 17482–17489.

Kirik, D., Annett, L. E., Burger, C., Muzyczka, N., Mandel, R. J., and Bjorklund, A. (2003). Nigrostriatal alpha-synucleinopathy induced by viral vector-mediated overexpression of human alpha-synuclein: a new primate model of Parkinson's disease. Proc. Natl. Acad. Sci. USA *100*, 2884–2889.

Kitada, T., Asakawa, S., Hattori, N., Matsumine, H., Yamamura, Y., Minoshima, S., Yokochi, M., Mizuno, Y., and Shimizu, N. (1998). Mutations in

the parkin gene cause autosomal recessive juvenile parkinsonism. Nature *392*, 605–608.

Kruger, R., Kuhn, W., Muller, T., Woitalla, D., Graeber, M., Kosel, S., Przuntek, H., Epplen, J. T., Schols, L., and Riess, O. (1998). Ala30Pro mutation in the gene encoding alpha-synuclein in Parkinson's disease. Nat. Genet. *18*, 106–108.

Lang, A. E., and Lozano, A. M. (1998). Parkinson's disease. Second of two parts. N. Engl. J. Med. *339*, 1130–1143.

Lashuel, H. A., Hartley, D., Petre, B. M., Walz, T., and Lansbury, P. T., Jr. (2002). Neurodegenerative disease: amyloid pores from pathogenic mutations. Nature *418*, 291.

Marx, F. P., *et al*. (2003). Identification and functional characterization of a novel R621C mutation in the synphilin-1 gene in Parkinson's disease. Hum. Mol. Genet. *12*, 1223–1231.

Masliah, E., Rockenstein, E., Veinbergs, I., Mallory, M., Hashimoto, M., Takeda, A., Sagara, Y., Sisk, A., and Mucke, L. (2000). Dopaminergic loss and inclusion body formation in alpha-synuclein mice: implications for neurodegenerative disorders. Science *287*, 1265–1269.

McLean, P. J., Kawamata, H., Shariff, S., Hewett, J., Sharma, N., Ueda, K., Breakefield, X. O., and Hyman, B. T. (2002). TorsinA and heat shock proteins act as molecular chaperones: suppression of alpha-synuclein aggregation. J. Neurochem. *83*, 846–854.

Outeiro, T. F., *et al*. (2007). Sirtuin 2 inhibitors rescue alpha-synuclein-mediated toxicity in models of Parkinson's disease. Science *317*, 516–519.

Outeiro, T. F., Putcha, P., Tetzlaff, J. E., Spoelgen, R., Koker, M., Carvalho, F., Hyman, B. T., and McLean, P. J. (2008). Formation of toxic oligomeric alpha-synuclein species in living cells. PLoS ONE *3*, e1867.

Pandey, U. B., *et al*. (2007). HDAC6 rescues neurodegeneration and provides an essential link between autophagy and the UPS. Nature *447*, 859–863.

Periquet, M., Fulga, T., Myllykangas, L., Schlossmacher, M. G., and Feany, M. B. (2007). Aggregated alpha-synuclein mediates dopaminergic neurotoxicity in vivo. J. Neurosci. *27*, 3338–3346.

Polymeropoulos, M. H., *et al*. (1996). Mapping of a gene for Parkinson's disease to chromosome 4q21–q23. Science *274*, 1197–1199.

Polymeropoulos, M. H., *et al*. (1997). Mutation in the alpha-synuclein gene identified in families with Parkinson's disease. Science *276*, 2045–2047.

Rong, Y. S., and Golic, K. G. (2000). Gene targeting by homologous recombination in *Drosophila*. Science *288*, 2013–2018.

Sharon, R., Bar-Joseph, I., Frosch, M. P., Walsh, D. M., Hamilton, J. A., and Selkoe, D. J. (2003). The formation of highly soluble oligomers of alpha-synuclein is regulated by fatty acids and enhanced in Parkinson's disease. Neuron *37*, 583–595.

Singleton, A. B., *et al*. (2003). alpha-Synuclein locus triplication causes Parkinson's disease. Science *302*, 841.

Taylor, J. P., Hardy, J., and Fischbeck, K. H. (2002). Toxic proteins in neurodegenerative disease. Science *296*, 1991–1995.

Taylor, J. P., Tanaka, F., Robitschek, J., Sandoval, C. M., Taye, A., Markovic-Plese, S., and Fischbeck, K. H. (2003). Aggresomes protect cells by enhancing the degradation of toxic polyglutamine-containing protein. Hum. Mol. Genet. *12*, 749–757.

Tu, P. H., Galvin, J. E., Baba, M., Giasson, B., Tomita, T., Leight, S., Nakajo, S., Iwatsubo, T., Trojanowski, J. Q., and Lee, V. M. (1998). Glial cytoplasmic inclusions in white matter oligodendrocytes of multiple system atrophy brains contain insoluble alpha-synuclein. Ann. Neurol. *44*, 415–422.

Wang, Z., Pan, Y., Li, W., Jiang, H., Chatzimanolis, L., Chang, J., Gong, Z., and Liu, L. (2008). Visual pattern memory requires foraging function in the central complex of *Drosophila*. Learn. Mem. *15*, 133–142.

Xu, J., Wei, C., Xu, C., Bennett, M. C., Zhang, G., Li, F., and Tao, E. (2007). Rifampicin protects PC12 cells against MPP+-induced apoptosis and inhibits the expression of an alpha-Synuclein multimer. Brain Res. *1139*, 220–225.

Yu, W. H., Dorado, B., Figueroa, H. Y., Wang, L., Planel, E., Cookson, M. R., Clark, L. N., and Duff, K. E. (2009). Metabolic activity determines efficacy of macroautophagic clearance of pathological oligomeric alpha-synuclein. Am. J. Pathol. *175*, 736–747.